Journal of Organometallic Chemistry 884 (2019) 36–43

Contents lists available at ScienceDirect

Journal of Organometallic Chemistry

journal homepage: www.elsevier.com/locate/jorganchem

Self-assembly of supramolecular coordination complexes based on half-sandwich metal corner with tunable host cavities

Peng Li [a], Yi-Mei Xu [a], Wei Deng [a, **], Zi-Jian Yao [a, b, *]

[a] School of Chemical and Environmental Engineering, Shanghai Institute of Technology, Shanghai, 201418, China
[b] Shanghai Key Laboratory of Molecular Catalysis and Innovative Material, State Key Laboratory of Coordination Chemistry, Nanjing University, Shanghai, 200433, China

ARTICLE INFO

Article history:
Received 3 November 2018
Received in revised form
17 January 2019
Accepted 30 January 2019
Available online 1 February 2019

Keywords:
Ruthenium
Supramolecular coordination complexes
Self-assembly
Host-guest systems

ABSTRACT

A dinuclear Ru(II) complex with the Ru-Ru distance of 12.840(6) Å was generated by dimeric metal precursor [(*p*-cymene)$RuCl_2$]$_2$ with the ligand of 1,4-bis(dipyrromethan-5-yl)benzene. Two types of supramolecular coordination Ru(II) complexes, tetra-nuclear metallacycle (ring **2**) and hexa-nuclear metallacage (cage **3**), have been synthesized stepwisely by the reactions of the dinuclear Ru(II) complex with bidentate bridge ligand of 4,4′-dipyridy and tridentate bridge ligand of 2,4,6-tris(pyridine-4-yl)-1,3,5-traizine (TPT) under template-free condition. The supramolecular coordination complexes (SCCs) with large cavity can encapsulate one or two guests afforded two host-guest systems (anthracene⊂ring **2**, pyrene⊂cage **3**) smoothly. The two supramolecular coordination Ru(II) complexes and host-guest systems have been characterized by ^{1}H NMR, ^{1}H–^{1}H COESY NMR, ESI-MS, and UV-vis. The dinuclear Ru(II) complex were further confirmed by single-crystal X-ray analysis.

1. Introduction

The design and preparation of supramolecular coordination complexes (SCCs) has attracted widespread attention not only because of their aesthetic appeal [1,2], but also their potential applications in various fields, such as containers for molecular flasks [3], host-guest chemistry [4–6], drug delivery systems [7,8], sensors [9–11], catalysis [12,13] and biomedical applications [14–16]. Coordination-driven self-assembly is an efficient synthetic method providing access to SCCs with finite sizes and shapes. Different from cyclodextrin and crown ether, the geometries of the coordination-driven self-assembly complexes structure can be easily designed by modify the predetermined acceptor clips and organic bridge ligands [17,18]. Owing to the good directionality and reversibility of metal–ligand coordination interaction, a large quantity of two dimensional (2D) metallacycles and three dimensional (3D) metallacages were reported in past decades [18–21], including the fascinating structures of triangles [14,22,23], squares [24], cubes [25], spheres [26,27], prisms [28,29], hexagons [30,31] and diamond-type shapes [32,33].

Among the various types of SCCs, the multicomponent self-assembly complexes constructed from platinum (Pt) or palladium (Pd) nodes have been extensively explored by Fujita group [34–36], which have been used as hosts for aromatics through π-π stacking interaction. When the aromatic molecules are encapsulated, the physicochemical properties of guest were expected significantly different from their free form. In contrast, two component supramolecular complexes with half-sandwich Ir(III) [37–39], Rh(III) [40–43], Ru(II) [44–47] fragments have also been designed and used to host small organic molecules. In particular, Ru-based compounds exhibit exciting application in biomedicine, represented by NAMI-A, KP1339, and RAPTA-C are progressing towards clinical trials as potential anticancer drugs [48]. The favorable biological activity has stimulated tremendous interesting to construct Ru metallosupramolecular complexes. Since 2008, Bruno [7,8,15,49,50] and other groups [51–53] have synthesized numerous arene Ru-based coordination cages, which have been used as a host for carry porphin [54] and other guest molecules to cancers tissues to enhanced permeablility and retention effect (EPR effect). According to the excellent studies, if the molecular and size of the arene Ru-based coordination complexes are enough big, the EPR effect would be effective enhanced [15]. Therefore, and all components have been used to increase the molecular weight and

* Corresponding author. School of Chemical and Environmental Engineering, Shanghai Institute of Technology, Shanghai, 201418, China.
** Corresponding author.
E-mail address: zjyao@sit.edu.cn (Z.-J. Yao).

https://doi.org/10.1016/j.jorganchem.2019.01.022
0022-328X/

size of the Ru-based supramolecular complexes upon functionalization, including also the guest molecule.

Indeed, some efforts to increase the molecular weight of guest have paid, and several pyrenyl-functionalized compounds have been used as guest moleculars to increase the molecular weight of Ru-based supramolecular complexes [55–58]. The pyrenyl group fits in the cavity of the Ru-based supramolecular complexes, while the remaining part sits outside. The combined components molecular have big weight, but the outside part has blocked the passage for the transport of guest molecules, which decrease application in drug delivery systems [59]. Thus, assembly of new Ru-based supramolecular complexe, which can provide huge cavities and permit two and more guests inside, is a more reasonable idea [55]. Although an Ru-cornered prismatic cage capable of encapsulating two molecules of coronene has been reported in 2010 [60], there are a few Ru-based supramolecular complexes with relatively huge cavities permit two and more guests inside.

Herein, based on a dinuclear Ru(II) complex with the metal–metal distance of 12.840(6) Å, two types of Ru(II) supramolecular complexes, including a tetra-nuclear metallacycle (ring **2**) and a hexa-nuclear metallacage (cage **3**), were obtained via self-assembly. The coordination-driven self-assembly complexes with tunable host cavity can encapsulate one or two guests smoothly. The two supramolecular coordination Ru(II) complexes have been characterized by ^{1}H NMR, ^{1}H–^{1}H COESY NMR and ESI-MS. The dinuclear Ru(II) complex were further confirmed by single-crystal X-ray analysis.

2. Results and discussion

The ligand of 1,4-bis(dipyrromethan-5-yl)benzene have been synthesized following the method reported by Lee *et al* [61]. The ligand readily formed the dinuclear arene Ru(II) acceptor clip **1** in moderate yield, by treating with 2,3-dichloro-5,6-dicyano-1,4-benzoquinone (DDQ), NaH and $[(p\text{-cymene})RuCl_2]_2$ under an atmosphere of nitrogen (Scheme 1). The formation of dinuclear Ru fragment was indicated by the ^{1}H NMR spectroscopy, ^{13}C NMR (ESI) and further confirmed by single-crystal X-ray analysis.

Suitable single crystal of dinuclear complex **1** (Fig. 1) was obtained by the slow diffusion of n-hexane into a saturated solution in dichloromethane. The air and thermal stability of the Ru complex can attribute to the two six-membered rings. The six-membered ring Ru(1)–N(1)–C(4)–C(5)–C(6)–N(2) of the dinuclear complex **1** is almost planar with the dihedral angle of 1.8° between planes of N(2)–Ru(1)–N(1) and C(4)–C(5)–C(5). The plane of the phenyl group is not perpendicular to the plane of the six-membered ring Ru(1)–N(1)–C(4)–C(5)–C(6)–N(2), the angle between these two planes is 66.4°. Particularly, the Ru…Ru distance of the dinuclear complex **1** is 12.840(6) Å, which is approximately four times the distance of π-π stacking [62]. Such a typical parameter had stimulated the interest to construct SCCs based on the dinuclear Ru complex **1**.

With the presence of silver triflate, treatment of bidentate ligand of 4,4′-dipyridy or tridentate ligand of 2,4,6-tris(pyridine-4-yl)-1,3,5-traizine (TPT) with dinuclear Ru complex **1** in CH_3OH under a nitrogen atmosphere for 24 h led to the formation of self-assembled Ru-based supramolecular metallacycle **2** or metallacage **3**, respectively (Scheme 2). The formation of metallacycle and metallacage was characterized by ^{1}H NMR spectra, ^{1}H-^{1}H COESY NMR spectra and electrospray ionization mass (ESI-MS) spectrometry.

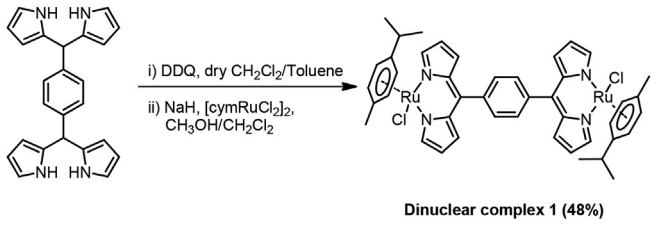

Scheme 1. Synthesis of the dinuclear Ru(II) complex **1**.

As shown in Fig. 2, in comparison with complex **1**, the ^{1}H NMR signals of *b*- and *c*-pyrrole protons (H_b, H_c) are slightly shifted, while the signal of *a*-pyrrole protons (H_a) is dramatically changed. Because of the coordination interaction between N and Ru atoms, the signals of α- and β-pyridyl protons (H_α, H_β) shifted upfield as compared of that of in free ligand of **L1** and **L2**. The aromatic protons of *p*-cymene moieties ($H_{p\text{-cymene}}$) in dinuclear complex **1** is one set of multiplet at 5.33 ppm, but the aromatic protons in the **2** and **3** are observed as two doublets (5.87, 6.27 ppm for **2**, 5.91, 6.34 ppm for **3**). Furthermore, the ^{1}H NMR spectrum of complex **1** showed a singlet peak at 7.44 ppm assigned by the phenyl protons (H_{Ph}) have split into two singlets at 6.69 (H_{Ph1}), 7.35 (H_{Ph2}) ppm of ring **2** and 6.64 (H_{Ph1}), 7.38 ppm (H_{Ph2}) of cage **3**, respectively. The significant changes were also supported by ^{1}H–^{1}H COESY NMR spectra. The ^{1}H–^{1}H COESY NMR spectra of ring **2** (Fig. 3, left) and cage **3** (Fig. 3, right) clearly show nuclear overhauser effects between the phenyl protons of H_{Ph1} and H_{Ph2}. The noticeable shift can be ascribed to the hindered rotation of the phenyl bridging ligand, which indicating the rigidity of the SCCs structure in solution [63].

In order to further confirm the formation of the two SCCs, electrospray ionization mass spectrometry (ESI-MS) were recoded. The electrospray ionization mass spectrometry spectra of the ring **2** showed a characteristic dicationic peak at *m/z* 494.12 corresponding to the fragment which lost two triflate anion ($[M_2-2CF_3SO_3]^{2+}$) (Fig. 4, left). The ESI-MS of cage **3** showed characteristic peak at *m/z* 519.62 corresponding to loss six triflate anion ($[M_3-3CF_3SO_3]^{3+}$) (Fig. 4, right). The peaks are good in agreement with the calculated theoretical distributions.

With the SCCs in hand, we next explored the ability of encapsulate electron-rich guests into the cavity of ring **2** and cage **3** to generate the inclusion complexes. To a CH_3OH solution of the SCCs was taken in a reaction vial, electron-rich guest (3 mol eq.) was added, anthracene for ring **2** and pyrene for cage **3**, respectively (Scheme 3). After stirred at room temperature for two hours, the solution was concentrated under vacuum to remove solvent, and the residue was washed with diethyl ether to get rid of the excess of guests. The formation of the two inclusion complexes were confirmed by ^{1}H NMR spectra, mass spectrometry and UV-visible spectroscopic analysis.

As shown in Fig. 5, due to the guest of anthracene into the cavity, the signals in ^{1}H NMR spectra were all shifted slightly between ring **2** and $G_1\subset$ring **2** (Scheme 3). In comparison with the^{1}H NMR spectrum of ring **2**, the signal of β-pyridyl protons (H_β) were shifted upfield in the ^{1}H NMR spectrum of $G_1\subset$ring **2**, while the ^{1}H NMR signals of *b*-pyrrole (H_b) and phenyl protons (H_{Ph}) were shifted downfield. Moreover, the single peak at 8.45 ppm (H_d) of free anthracene split into a doublet at 8.35 ppm in $G_1\subset$ring **2**, which indicating the protons of H_d in guest have been influenced by the α-pyridyl protons (H_α) of host.

Similarly, for inclusion complex of $G_2\subset$cage **3**, the ^{1}H NMR signals of α- and β-pyridyl protons (H_α, H_β) were shifted upfield, the signals associated with pyrrole (H_a, H_b, H_c) and phenyl protons (H_{Ph}) were shifted downfield (Fig. 6). The signals of pyrene (H_o, H_p, H_q) in the inclusion complex were shifted upfield clearly compared to the free pyrene. The change of the chemical shift indicated the guest of pyrene had been encapsulated into the cavity of cage **3**. As observed previously, due to the localization at the periphery of the

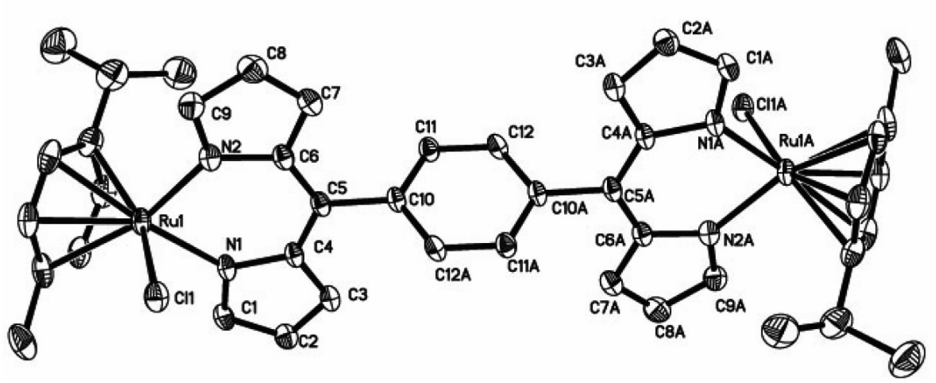

Fig. 1. X-ray crystal structures of dinuclear Ru(II) complex **1**. All hydrogen atoms are omitted for clarity. Selected bond length (Å) and angles (°): Ru-Ru, 12.8403(6); Ru(1)-N(2), 2.080(3); Ru(1)-N(1), 2.084(2); Ru(1)-Cl(1), 2.4191(8); N(2)-Ru(1)-N(1), 86.64(10); N(2)-Ru(1)-Cl(1), 85.85(7); N(1)-Ru(1)-Cl(1), 83.84(7); C(9)-N(2)-Ru(1), 124.7(2); C(1)-N(1)-Ru(1), 124.57(19); C(4)-N(1)-Ru(1), 129.0(2); C(6)-N(2)-Ru(1), 129.0(2); C(6)-C(5)-C(4), 126.3(3).

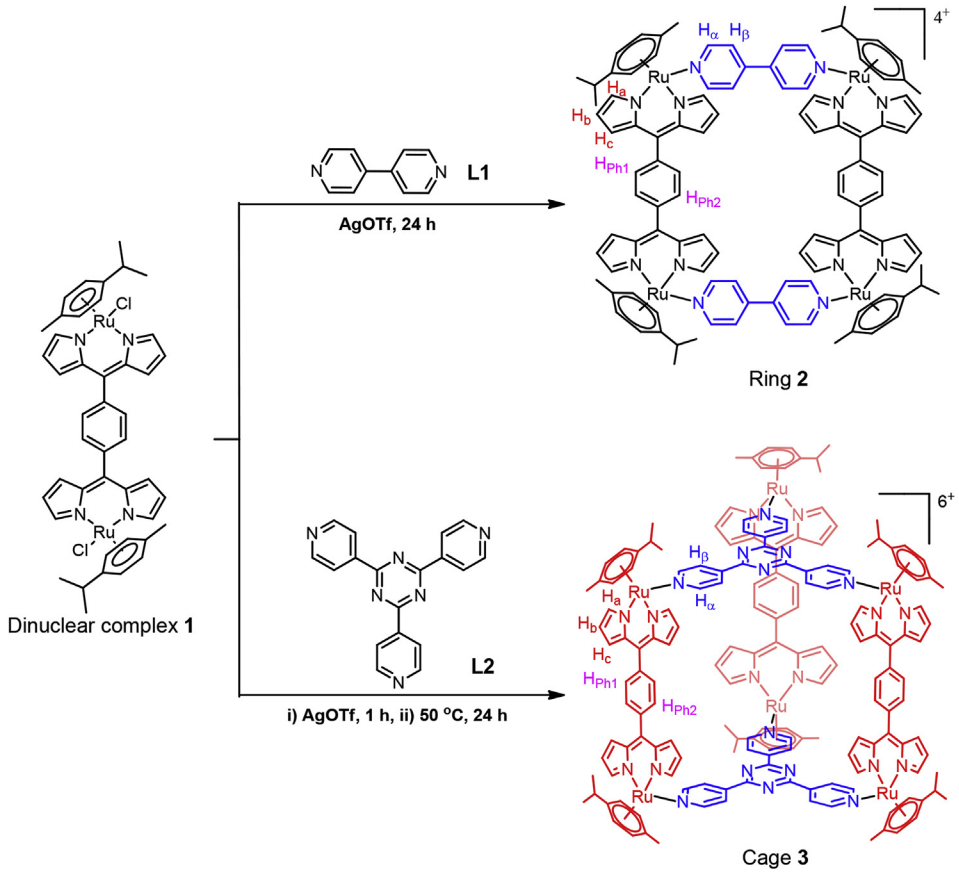

Scheme 2. Self-assembly of ring **2** and cage **3**.

SSCs, the signals of the *p*-cymene protons were not obvious influence by the presence of guests inside to the cavity [64].

The formation of the two inclusion complexes were supported by the electrospray ionization mass spectrometry spectrum. The ESI-MS spectrum of $G_1\subset$ring **2** show a signal at *m/z* 1225.72, corresponding to loss two triflate anions: ($[M_2+\text{anthracene}-2CF_3SO_3]^{2+}$) (Fig. 7, left). And a charged state at *m/z* 955.20 in the ESI-MS spectrum of the $G_2\subset$cage **3**, which corresponding to loss four triflate anions: ($[M_3+2\text{pyrene}-4CF_3SO_3]^{4+}$) (Fig. 7, right).

In order to further confirm the formation of inclusion complexes of $G_1\subset$ring **2** and $G_2\subset$cage **3**, the UV-visible spectroscopic analysis were recorded. The UV-visible absorption spectra of the all SCCs (Fig. 8) have shown a band at around 295 nm, which matched with a ligand-localized or intraligand π-π^* transition, as well as broad low-energy bands related to metal-to-ligand charge transfer (MLCT) transitions [62]. In addition, as compared to the absorption of the empty metallacycle, the inclusion complex of $G_1\subset$ring **2** showed two new absorption peaks at 355 nm and 375 nm assigned to the guest of anthracene, indicating the guest had been encapsulated into the metallacycle. Likewise, in the inclusion complex of $G_2\subset$cage **3**, two obvious additional absorption peaks at 320 nm and 333 nm consistent with the spectra of free pyrene, which associated

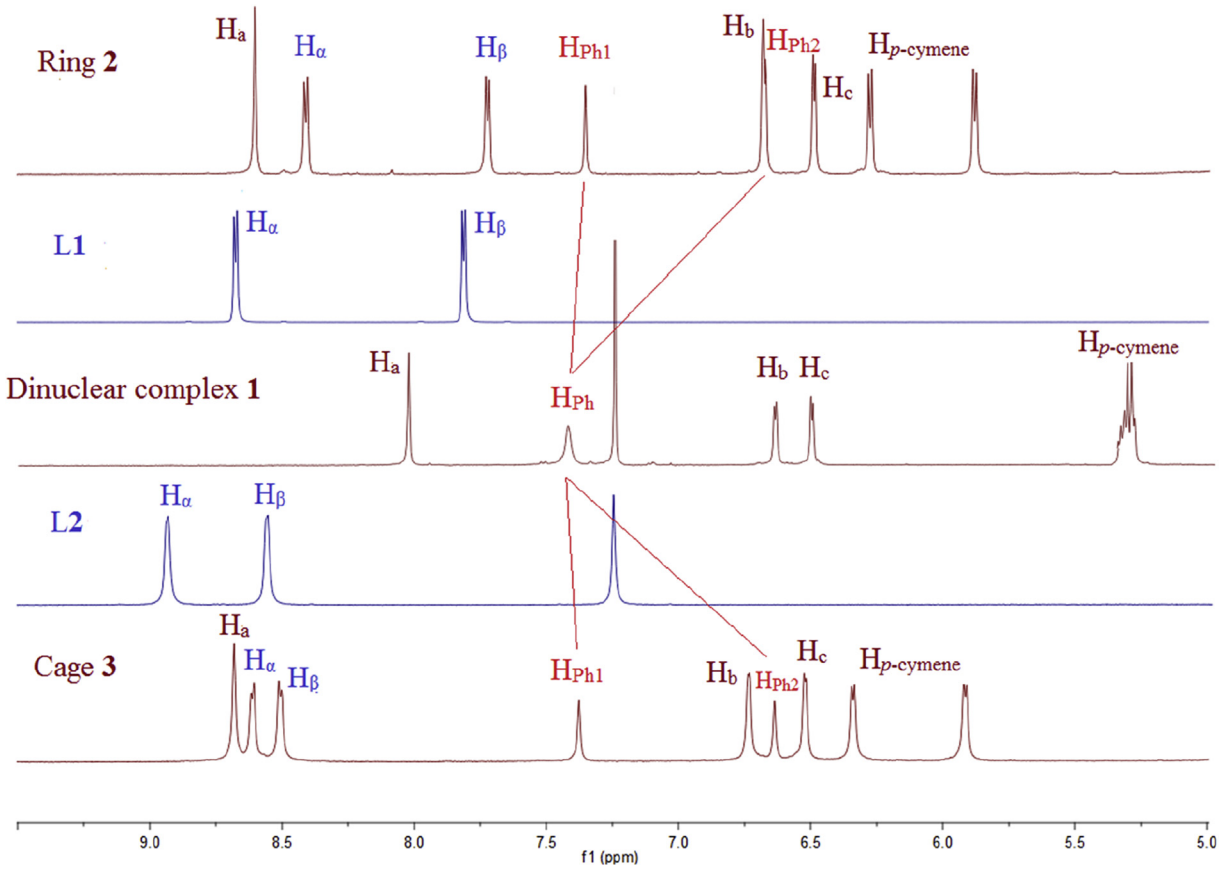

Fig. 2. The ^{1}H NMR spectra of complex **1**, 4,4′-dipyridy (**L1**), TPT (**L2**), ring **2** and cage **3**.

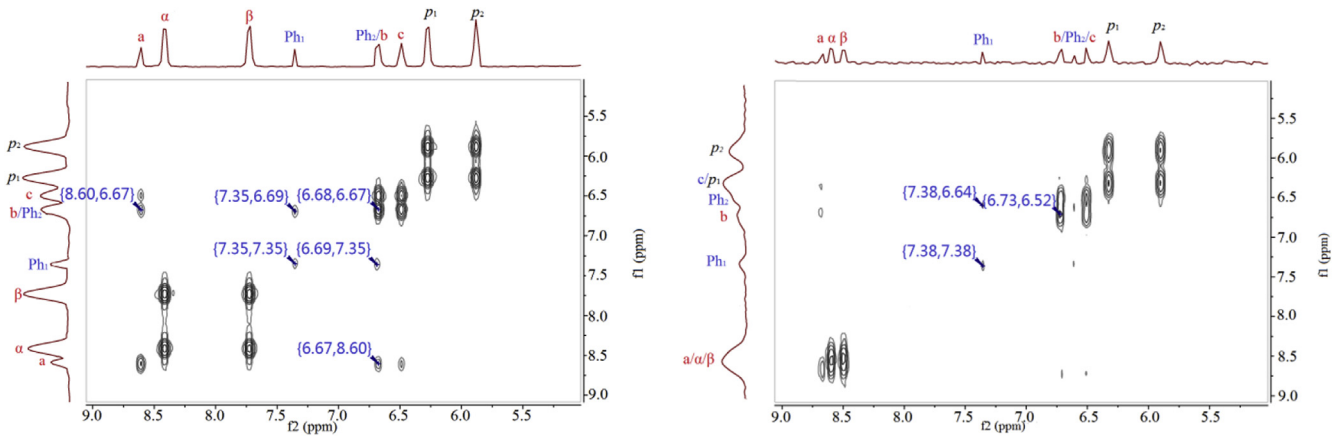

Fig. 3. The ^{1}H−^{1}H COESY NMR spectra of ring **2** (left) and cage **3** (right).

with the pyrene within the cavity of cage **3**.

3. Conclusions

In conclusion, a dinuclear Ru complex with the Ru-Ru distance of 12.840(6) Å had been designed. Based on the dinuclear Ru complex, two types of supramolecular coordination Ru(II) complexes, including a tetra-nuclear metallacycle (ring **2**) and a hexa-nuclear metallacage (cage **3**), had been synthesized by self-assembly under template-free condition. Unlike the most reported SCCs, the two Ru-based supramolecular complexes with tunable host cavity can encapsulate one or two electron-rich planar guests smoothly through π-π stacking interactions. The above evidence strong suggested the formation of the inclusion complexes. The biological applications of the SCCs carry the drug molecules to tissues and cells are underway in our laboratory.

4. Experimental section

The ligands of 1,4-bis(dipyrromethan-5-yl)benzene and 2,4,6-tris(pyridine-4-yl)-1,3,5-traizine (TPT) have been synthesized following the reported procedures [61,65]. All manipulations were

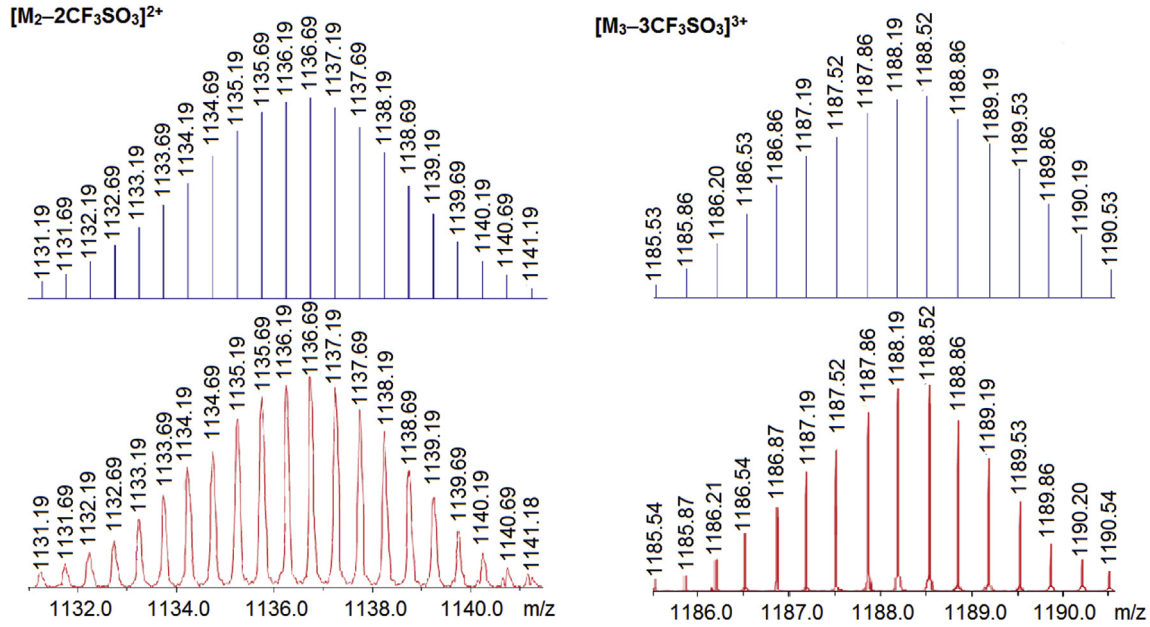

Fig. 4. Calculated (blue) and experimental (red) ESI-MS spectra of the ring **2** (left) and cage **3** (right). (For interpretation of the references to colour in this figure legend, the reader is referred to the Web version of this article.)

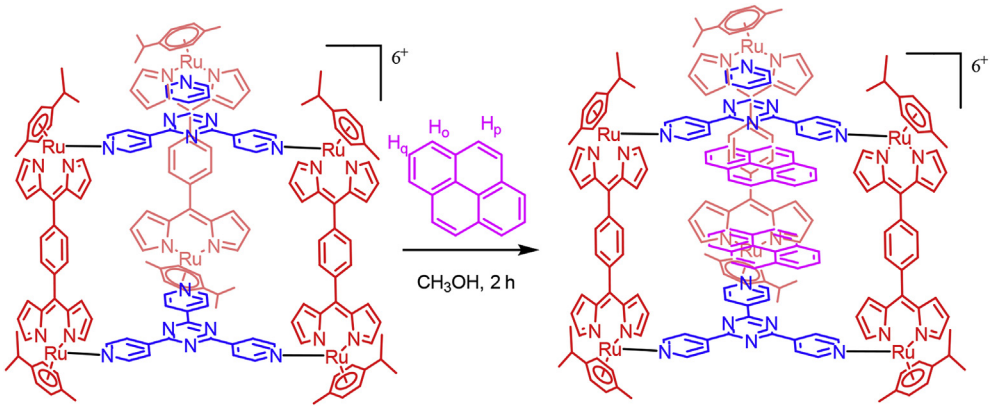

Scheme 3. Synthesis of $G_1 \subset$ ring **2** and $G_2 \subset$ cage **3**.

performed under an atmosphere of nitrogen using standard Schlenk techniques. The solvents were all dried and distilled from calcium hydride. Other chemicals were used as commercial products without further purification. ^{1}H NMR (500 MHz), ^{13}C NMR (125 MHz) and ^{1}H–^{1}H COSY NMR spectra were recorded with a Bruker DMX-500 spectrometer. Mass spectra were recorded on a Waters API Quattro Micro triple-quadrupole mass spectrometer in the positive ion mode. UV/Visible absorption spectra were recorded using a UV 765 spectrophotometer with quartz cuvettes of 1 cm path length.

Synthesis of dinuclear complex ***1***: To a solution of 1,4-bis-(dipyrromethan-5-yl)-benzene (0.1 mmol, 36.6 mg) in dry CH_2Cl_2 was added a solution of DDQ (0.22 mmol, 50.0 mg) in dry toluene drop by drop under ice bath. The mixture was stirred at 0 °C for 10 min, and then allowed to warm to room temperature for 2 h. The solvent was removed under reduced pressure, and the resulting red solid was removed to a Schlenk flask. NaH (0.22 mmol, 5.28 mg) and [*p*-Cymene $RuCl_2]_2$ (0.1 mmol, 61.2 mg) were added, and the mixture was stirred in dry CH_2Cl_2/CH_3OH for 8 h under a nitrogen atmosphere at room temperature. The mixture was filtered and evaporated to give the crude products which were further purified by silica gel column chromatography (CH_2Cl_2: CH_3OH = 50: 1) to afford pure product of dinuclear complex **1** as a red solid. Yield: 48% (46.8 mg). ^{1}H NMR (500 MHz, $CDCl_3$) δ (ppm) 8.04 (s, 4H, pyrrole–H_a), 7.44 (s, 4H, Ph–*H*), 6.66 (d, J = 4.0 Hz, 4H, pyrrole–H_b), 6.52 (d, J = 3.5 Hz, 4H, pyrrole–H_c), 5.36–5.31 (m, 8H, *p*-cymene–*H*), 2.50–2.43 (m, 2H, C*H*$(CH_3)_2$), 2.25 (s, 6H, Ph–CH_3), 1.11 (d, J = 7.0 Hz, 16H, CH_3). ^{13}C NMR (125 MHz, $CDCl_3$) δ 155.12 (s, 4C), 145.90 (s, 2C), 138.24 (s, 2C), 135.18 (s, 2C), 132.60 (s, 2C), 131.08 (s, 4C), 128.72 (s, 2C), 118.63 (s, 4C), 117.33 (s, 2C), 108.46 (s, 2C), 107.22 (s, 2C), 85.08 (s, 4C), 84.66 (s, 4C), 30.74 (s, 2C), 22.23 (s, 4C), 18.72 (s, 2C). Elemental analysis calcd (%) for $C_{44}H_{44}Cl_2N_4Ru_2$: C 58.60, H 4.92, N 6.21; found: C 58.69, H 4.90, N 6.26.

Synthesis of ring ***2***: In a Schlenk flask, a mixture of the dinuclear complex **1** (0.05 mmol, 48.8 mg), $AgCF_3SO_3$ (0.15 mmol, 38.5 mg) and ligand of 4,4′-dipyridy (0.06 mmol, 9.37 mg) was stirred in 15 mL of CH_2Cl_2/CH_3OH (1:1) for 8 h under a nitrogen atmosphere in the dark at room temperature. The mixture was filtered, and the solvent was removed under reduced pressure. The crude product was dissolved in CH_3OH, and then diethyl ether was added,

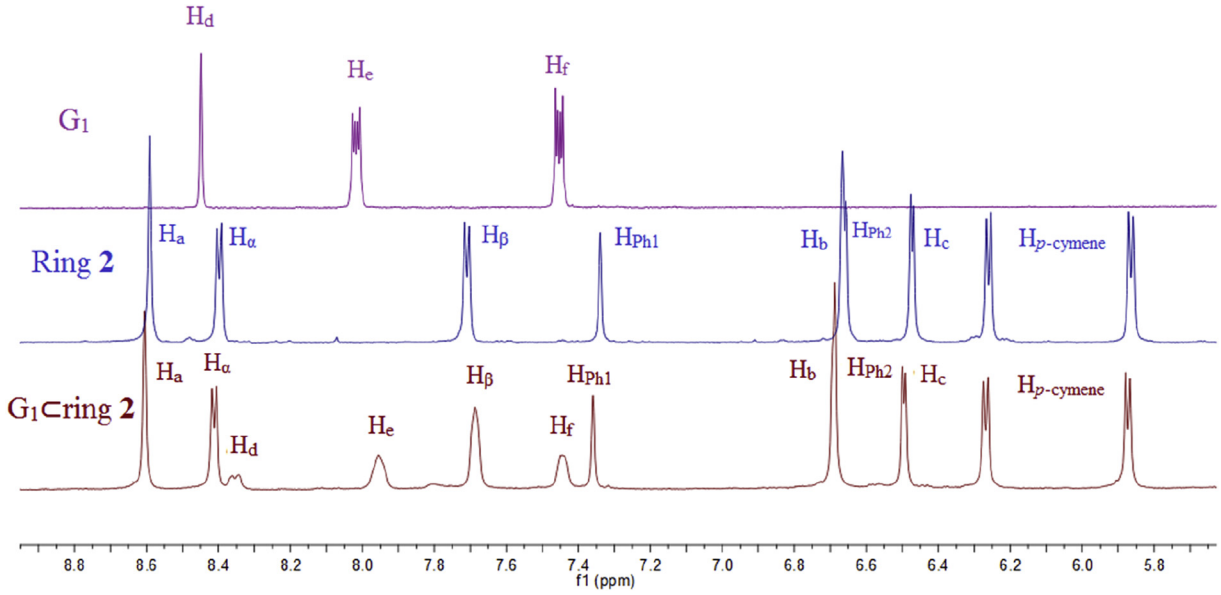

Fig. 5. The comparison of ^{1}H NMR spectra of anthracene (G_1), ring **2** and $G_1\subset$ring **2** in CD_3OD.

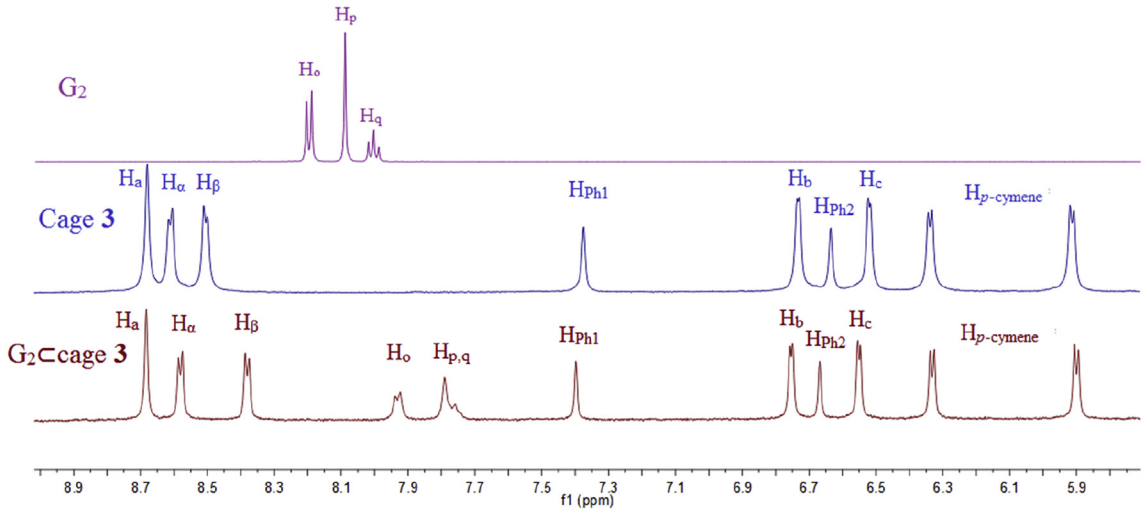

Fig. 6. The comparison of ^{1}H NMR spectra of pyrene (G_2), cage **3** and $G_2\subset$cage **3** in CD_3OD.

precipitated, and collected by filtration to afford a red brown solid. Yield: 80% (51.4 mg). ^{1}H NMR (500 MHz, CD_3OD) δ (ppm) 8.60 (s, 8H, pyrrole−H_a), 8.40 (d, $J = 6.5$ Hz, 8H, dipyridy−H_α), 7.72 (d, $J = 6.5$ Hz, 8H, dipyridy−H_β), 7.34 (s, 4H, Ph−H), 6.67 (d, $J = 5.0$ Hz, 8H, pyrrole−H_b; 4H, Ph−H), 6.48 (d, $J = 4.0$ Hz, 8H, pyrrole−H_c), 6.27 (d, $J = 6.0$ Hz, 8H, *p*-cymene−H), 5.87 (d, $J = 6.5$ Hz, 8H, *p*-cymene−H), 2.45−2.40 (m, 4H, $CH(CH_3)_2$), 1.77 (s, 12H, Ph−CH_3), 0.99 (d, $J = 7.0$ Hz, 24H, CH_3). ESI-MS: calcd for $C_{110}H_{104}F_6N_{12}O_6Ru_4S_2$ $[M_2-2CF_3SO_3]^{2+}$: 1136.69, found: 1136.69.

Synthesis of cage ***3***: A mixture of the dinuclear complex **1** (0.06 mmol, 58.6 mg) and $AgCF_3SO_3$ (0.20 mmol, 51.38 mg) was stirred in 15 mL of CH_2Cl_2/CH_3OH (1:1) for 4 h in the dark at room temperature. AgCl was filtered off, and the solvent was removed under reduced pressure. The residue and TPT (0.05 mmol, 15.6 mg) was added to a Schlenk flask, and the mixture was stirred in 15 mL of CH_3OH for 24 h at 60 °C under a nitrogen atmosphere. The mixture was filtered, and the solvent was evaporated to 2 mL under reduced pressure. Then, diethyl ether was added, precipitated, and collected by filtration to afford a red brown solid. Yield: 68% (57.6 mg). ^{1}H NMR (500 MHz, CD_3OD) δ (ppm) 8.68 (s, 12H, pyrrole−H_a), 8.61 (d, $J = 5.5$ Hz, 12H, dipyridy−H_α), 8.51 (d, $J = 5.0$ Hz, 12H, dipyridy−H_β), 7.38 (s, 6H, Ph−H), 6.73 (d, $J = 3.5$ Hz, 12H, pyrrole−H_b), 6.64 (s, 6H, Ph−H), 6.52 (d, $J = 3.0$ Hz, 12H, pyrrole−H_c), 6.34 (d, $J = 5.5$ Hz, 12H, *p*-cymene−H), 5.92 (d, $J = 6.0$ Hz, 12H, *p*-cymene−H), 2.51−2.45 (m, 6H, $CH(CH_3)_2$), 1.77 (s, 18H, Ph−CH_3), 1.04 (d, $J = 7.0$ Hz, 36H, CH_3). ESI-MS: calcd for $C_{171}H_{156}F_9N_{24}O_9Ru_6S_3$ $[M_3-3CF_3SO_3]^{3+}$: 1188.52, found: 1188.52.

Synthesis of $G_1\subset$*ring* ***2***: To a solution of the ring **2** (0.005 mmol, 12.8 mg) and anthracene (0.015 mmol, 2.7 mg) in CH_3OH was taken in a reaction vial, and stirred for 2 h at room temperature. The solvent removed under reduced pressure, washed with diethyl ether to get rid of the excess of guests to afford a red brown solid. Yield: 96% (13.1 mg). ^{1}H NMR (500 MHz, CD_3OD) δ (ppm) 8.61 (s, 8H, pyrrole−H_a), 8.41 (d, $J = 6.5$ Hz, 8H, dipyridy−H_α), 8.35 (d, $J = 11.0$ Hz, 2H, anthracene−H_d), 7.98−7.93 (m, 4H, anthracene−H_e), 7.69 (s, 8H, dipyridy−H_β), 7.44 (d, $J = 6.0$ Hz, 4H, anthracene−H_f),

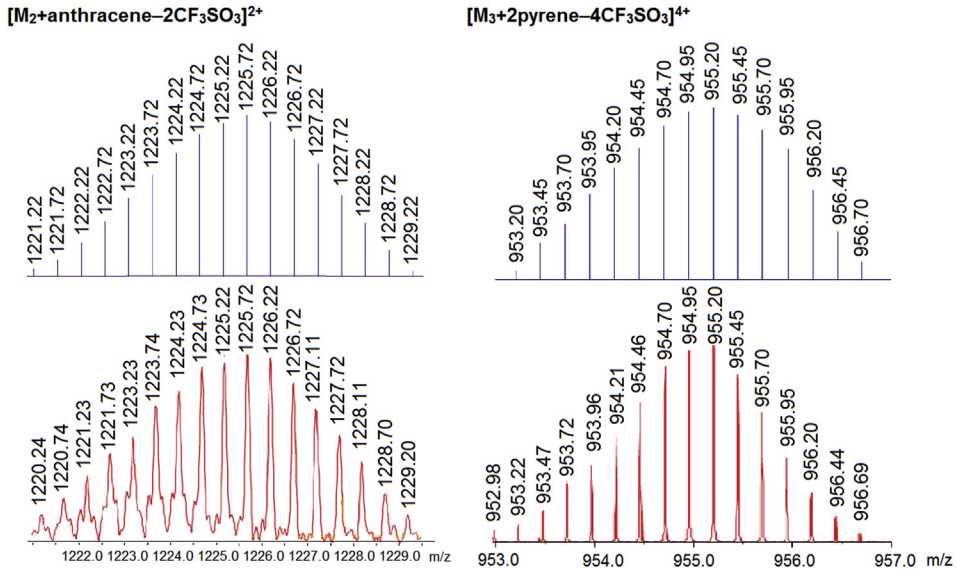

Fig. 7. Calculated (blue) and experimental (red) ESI-MS spectra of the $G_1\subset$ring **2** (left) and $G_2\subset$cage **3** (right). (For interpretation of the references to colour in this figure legend, the reader is referred to the Web version of this article.)

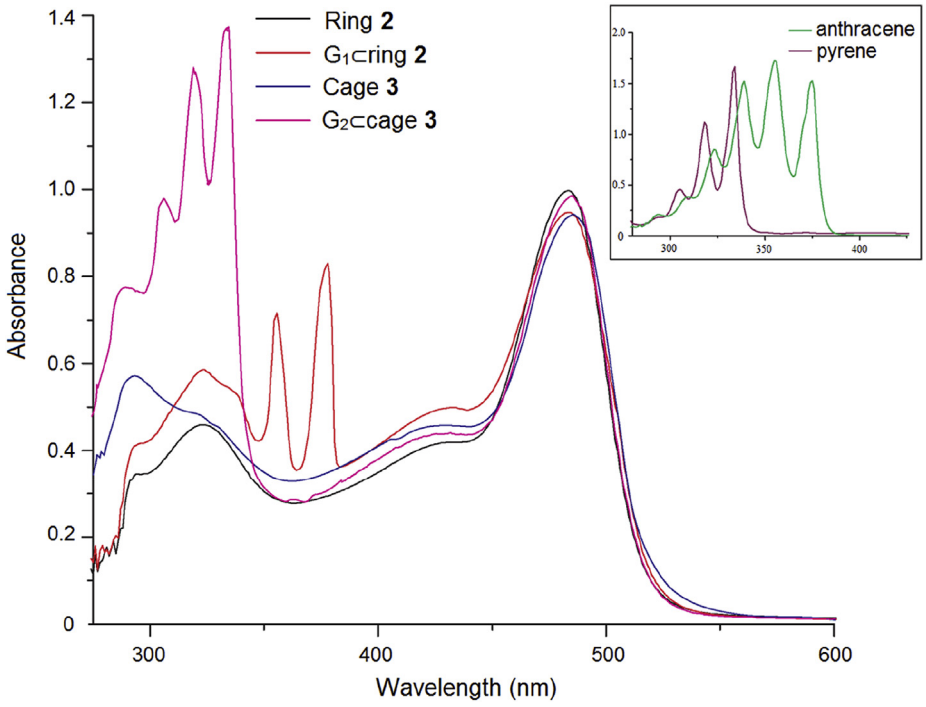

Fig. 8. UV absorption of the ring **2**, cage **3**, $G_1\subset$ ring **2** and $G_2\subset$cage **3** (the inset showing the spectra of G_1 and G_2) in CH_3OH at room temperature. ($c = 1.0 \times 10^{-5}$ M).

7.36 (s, 4H, Ph–*H*), 6.69 (s, 8H, pyrrole–H_b; 4H, Ph–*H*), 6.50 (d, $J = 4.0$ Hz, 8H, pyrrole–H_c), 6.27 (d, $J = 6.0$ Hz, 8H, *p*-cymene–*H*), 5.87 (d, $J = 6.0$ Hz, 8H, *p*-cymene–*H*), 2.43 (m, 4H, $CH(CH_3)_2$), 1.78 (s, 12H, Ph–CH_3), 1.01 (d, $J = 7.0$ Hz, 24H, CH_3). ESI-MS: calcd for $C_{124}H_{104}F_6N_{12}O_6Ru_4S_2$ $[M_2+\text{anthracene}-2CF_3SO_3]^{2+}$: 1225.72, found: 1225.72.

Synthesis of $G_2\subset$cage **3**: To a solution of the cage **3** (0.005 mmol, 21.2 mg) and pyrene (0.015 mmol, 3.0 mg) in CH_3OH was taken in a reaction vial, and stirred for 2 h at room temperature. The solvent removed under reduced pressure, washed with diethyl ether to get rid of the excess of guests to afford a red brown solid. Yield: 98% (22.7 mg). ^{1}H NMR (500 MHz, CD_3OD) δ (ppm) 8.68 (s, 12H, pyrrole–H_a), 8.58 (d, $J = 6.0$ Hz, 12H, dipyridy–H_α), 8.38 (d, $J = 6.0$ Hz, 12H, dipyridy–H_β), 7.93 (d, $J = 6.5$ Hz, 8H, pyrene–H_o), 7.79–7.75 (m, 4H, pyrene–H_p; 8H, pyrene–H_q), 7.40 (s, 6H, Ph–*H*), 6.75 (d, $J = 3.5$ Hz, 12H, pyrrole–H_b), 6.67 (s, 6H, Ph–*H*), 6.55 (d, $J = 3.5$ Hz, 12H, pyrrole–H_c), 6.33 (d, $J = 6.0$ Hz, 12H, *p*-cymene–*H*), 5.90 (d, $J = 6.0$ Hz, 12H, *p*-cymene–*H*), 2.48 (m, $J = 13.7$, 6.4 Hz, 6H, $CH(CH_3)_2$), 1.75 (s, 18H, Ph–CH_3), 1.04 (d, $J = 7.0$ Hz, 36H, CH_3). ESI-MS: calcd for $C_{202}H_{176}F_{12}N_{24}O_{12}Ru_6S_4$ $[M_3+2\text{pyrene}-4CF_3SO_3]^{4+}$: 955.20, found: 955.20.

Acknowledgement

This work was supported by National Natural Science Foundation of China (No. 21601125), Shanghai Municipal Education Commission (Plateau Discipline Construction Program), Natural Science Foundation of Shanghai (No. 16ZR1435700), and Start funding of Shanghai Institute of Technology (YJ2016-10).

Appendix A. Supplementary data

Supplementary data to this article can be found online at https://doi.org/10.1016/j.jorganchem.2019.01.022.

References

[1] H. Lee, P. Elumalai, N. Singh, H. Kim, S.U. Lee, K.W. Chi, J. Am. Chem. Soc. 137 (2015) 4674–4677.
[2] R. Chakrabarty, P.S. Mukherjee, P.J. Stang, Chem. Rev. 111 (2011) 6810–6918.
[3] Y. Inokuma, M. Kawano, M. Fujita, Nat. Chem. 3 (2011) 349–358.
[4] S. Li, J. Huang, T.R. Cook, J.B. Pollock, H. Kim, K.W. Chi, P.J. Stang, J. Am. Chem. Soc. 135 (2013) 2084–2087.
[5] Y.-F. Han, H. Li, G.-X. Jin, Chem. Commun. 46 (2010) 6879–6890.
[6] Q.-J. Fan, Y.-J. Lin, F.E. Hahn, G.-X. Jin, Dalton Trans. 47 (2018) 2240–2246.
[7] T. Bruno, Chem. Eur. J. 19 (2013) 8378–8386.
[8] T. Bruno, S.-F. Georg, G. Padavattan, R.K. Anna, D.J. Paul, Angew. Chem. Int. Ed. 47 (2008) 3773–3776.
[9] G. Gupta, A. Das, N.B. Ghate, T. Kim, J.Y. Ryu, J. Lee, N. Mandal, C.Y. Lee, Chem. Commun. 52 (2016) 4274–4277.
[10] J. Zhou, G. Yu, F. Huang, Chem. Soc. Rev. 46 (2017) 7021–7053.
[11] G. Gupta, A. Das, S. Panja, J.Y. Ryu, J. Lee, N. Mandal, C.Y. Lee, Chem. Eur. J. 23 (2017) 17199–17203.
[12] M. Yoon, R. Srirambalaji, K. Kim, Chem. Rev. 112 (2012) 1196–1231.
[13] A.N. Oldacre, A.E. Friedman, T.R. Cook, J. Am. Chem. Soc. 139 (2017) 1424–1427.
[14] J. Zhou, Y. Zhang, G. Yu, M.R. Crawley, C.R.P. Fulong, A.E. Friedman, S. Sengupta, J. Sun, Q. Li, F. Huang, T.R. Cook, J. Am. Chem. Soc. 140 (2018) 7730–7736.
[15] M. Vidya, T. Bruno, Inorg. Chem. 57 (2018) 3626–3633.
[16] T.R. Cook, V. Vajpayee, M.H. Lee, P.J. Stang, K.W. Chi, Acc. Chem. Res. 46 (2013) 2464–2474.
[17] Y.-F. Han, G.-X. Jin, Acc. Chem. Res. 47 (2014) 3571–3579.
[18] G. Anton, R.J. Thomas, S. Rosario, S. Kay, Angew. Chem. Int. Ed. 49 (2010) 5515–5518.
[19] Y.-F. Han, Y.-J. Lin, W.-G. Jia, L.-H. Weng, G.-X. Jin, Organometallics 26 (2007) 5848–5853.
[20] Y.-F. Han, W.-G. Jia, Y.-J. Lin, G.-X. Jin, Organometallics 27 (2008) 5002–5008.
[21] M. Wang, V. Vajpayee, S. Shanmugaraju, Y.R. Zheng, Z. Zhao, H. Kim, P.S. Mukherjee, K.W. Chi, P.J. Stang, Inorg. Chem. 50 (2011) 1506–1512.
[22] Y. Lu, Y.-X. Deng, Y.-J. Lin, Y.-F. Han, L.-H. Weng, Z.-H. Li, G.-X. Jin, Chem 3 (2017) 110–121.
[23] J. Heo, Y.,-M. Jeon, C.A. Mirkin, J. Am. Chem. Soc. 129 (2007) 7712–7713.
[24] P.B. Anais, P.E.B. Nicolas, R. Virginie, H. Benoit, D. Bertrand, T. Bruno, D. Robert, J. Am. Chem. Soc. 136 (2014) 17616–17625.
[25] M. Wang, Y.-R. Zheng, K. Ghosh, P.J. Stang, J. Am. Chem. Soc. 132 (2010) 6282–6283.
[26] D. Moon, S. Kang, J. Park, K. Lee, R.P. John, H. Won, G.H. Seong, Y.S. Kim, G.H. Kim, H. Rhee, M.S. Lah, J. Am. Chem. Soc. 128 (2006) 3530–3531.
[27] M. Tominaga, K. Suzuki, M. Kawano, T. Kusukawa, T. Ozeki, S. Sakamoto, K. Yamaguchi, M. Fujita, Angew. Chem. Int. Ed. 43 (2004) 5621–5625.
[28] G. Pasavattan, L. David, L. Jerome, S.F. Georg, T. Bruno, Dalton Trans. 0 (2007) 4457–4463.
[29] Y. Yamanoi, Y. Sakamoto, T. Kusukawa, M. Fujita, S. Sakamoto, K. Yamaguchi, J. Am. Chem. Soc. 123 (2001) 980–981.
[30] K. Ghosh, H.B. Yang, B.H. Northrop, M.M. Lyndon, Y.R. Zheng, D.C. Muddiman, P.J. Stang, J. Am. Chem. Soc. 130 (2008) 5320–5334.
[31] K. Ghosh, Y. Zhao, H.-B. Yang, B.H. Northrop, H.S. White, P.J. Stang, J. Org. Chem. 74 (2009) 4828–4833.
[32] T. Kusukawa, M. Fujita, J. Am. Chem. Soc. 124 (2002) 13576–13582.
[33] L. Cao, P. Wang, X. Miao, Y. Dong, H. Wang, H. Duan, Y. Yu, X. Li, P.J. Stang, J. Am. Chem. Soc. 140 (2018) 7005–7011.
[34] M. Yoshizawa, J. Nakagawa, K. Kumazawa, M. Nagao, M. Kawano, T. Ozeki, M. Fujita, Angew. Chem. Int. Ed. 44 (2005) 1810–1813.
[35] K. Ono, M. Yoshizawa, M. Akita, T. Kate, Y. Tsunobuchi, S. Ohkoshi, M. Fujita, J. Am. Chem. Soc. 131 (2009) 2782–2783.
[36] K. Harris, D. Fujita, M. Fujita, Chem. Commun. 49 (2013) 6703–6712.
[37] Y.-F. Han, L. Zhang, L.-H. Weng, G.-X. Jin, J. Am. Chem. Soc. 136 (2014) 14608–14615.
[38] Y.-F. Han, W.-G. Jia, Y.-J. Lin, G.-X. Jin, Angew. Chem. Int. Ed. 48 (2009) 6234–6238.
[39] H.-N. Zhang, W.-X. Gao, Y.-X. Deng, Y.-J. Lin, G.-X. Jin, Chem. Commun. 54 (2018) 1559–1562.
[40] Z. Grote, S. Bonazzi, R. Scopelliti, K. Severin, J. Am. Chem. Soc. 128 (2006) 10382–10383.
[41] Y.-F. Han, Y.-J. Lin, L.-H. Weng, H. Berke, G.-X. Jin, Chem. Commun. 0 (2008) 350–352.
[42] W.-X. Gao, Q.-J. Fan, Y.-J. Lin, G.-X. Jin, Chin. J. Chem. 36 (2018) 594–598.
[43] L. Zhang, L. Lin, D. Liu, Y.-J. Lin, Z.-H. Li, G.-X. Jin, J. Am. Chem. Soc. 139 (2017) 1653–1660.
[44] M. Johan, G. Padavattan, F. Julien, S. Yoshihisa, Y. Kentaro, S. Georg, T. Bruno, Organometallics 27 (2008) 4346–4356.
[45] K. Benan, M. Sebastian, R.J. Thomas, S. Rosario, S. Kay, Inorg. Chem. 51 (2012) 5795–5804.
[46] A. Mishra, A. Dubey, J.W. Min, H. Kim, P.J. Stang, K.W. Chi, Chem. Commun. 50 (2014) 7542–7544.
[47] S. Frederic, B.P.E. Nicolas, J.-J. Lucienne, T. Bruno, *Bioorg.* Med. Chem. Lett. 22 (2012) 178–180.
[48] C. Mari, V. Pierroz, S. Ferrari, G. Gasser, Chem. Sci. 6 (2015) 2660–2686.
[49] S. Frederic, G. Padavattan, Z. Olivier, S.-F. Georg, J.-J. Lucienne, T. Bruno, J. Biol. Inorg. Chem. 14 (2009) 101–109.
[50] T. Bruno, F. Julien, Adv. Chem. 2014 (2014) 1–20.
[51] A. Dubey, Y.J. Jeong, J.H. Jo, S. Woo, D.H. Kim, H. Kim, S.C. Kang, P.J. Stang, K.W. Chi, Organometallics 34 (2015) 4507–4514.
[52] T.R. Cook, Y.R. Zheng, P.J. Stang, Chem. Rev. 113 (2013) 734–777.
[53] A.K. Singh, D.S. Pandey, Q. Xu, P. Braunstein, Coord. Chem. Rev. 270–271 (2014) 31–56.
[54] G. Amine, J.P. Mbakid, C. Vincent, S. Vincent, O. Ersin, T. Bruno, Organometallics 34 (2015) 4138–4146.
[55] W.Y. Jeong, B.P.E. Nicolas, F.A. Mona, Z. Olivier, D.J. Paul, T. Bruno, H.K. Byeang, Bioconjug. Chem. 23 (2012) 461–471.
[56] P.B. Anais, P.E.B. Nicolas, Z. Olivier, D. Robert, J.D. Paul, T. Bruno, Chem. – Eur. J. 17 (2011) 1966–1971.
[57] T. Bruno, CrystEngComm 17 (2015) 484–491.
[58] A.F. Mona, S. Frederic, W. Michael, J.J. Lucienne, T. Bruno, Dalton Trans. 41 (2012) 7201–7211.
[59] A. Mishra, S.C. Kang, K.W. Chi, Eur. J. Inorg. Chem. (2013) 5222–5232, 2013.
[60] M. Sebastian, S.-T. Adam, S. Rosario, H.V. Aldrik, S. Kay, J. Am. Chem. Soc. 1323 (2010) 14004–14005.
[61] C.-H. Lee, J.S. Lindsey, Tetrahedron 50 (1994) 11427–11440.
[62] N. Singh, J.H. Jo, Y.-H. Song, H. Kim, D. Kim, M.S. Lah, K.W. Chi, Chem. Commun. 51 (2015) 4492–4495.
[63] G. Tarkany, H. Jude, G. Palinkas, P.J. Stang, Org. Lett. 7 (2005) 4971–4973.
[64] A.F. Mona, S. frederic, W. Michael, J.-J. Lucienne, T. Bruno, Dalton Trans. 41 (2012) 7201–7211.
[65] Z. He, M. Li, W. Que, P.J. Stang, Dalton Trans. 46 (2017) 3120–3124.